Eur. J. Mineral.
2003, **15**, 137–146

Crystal structure, cation ordering, and polytypic character of diaphorite, $Pb_2Ag_3Sb_3S_8$, a PbS-based structure

THOMAS ARMBRUSTER[1], EMIL MAKOVICKY[2], PETER BERLEPSCH[2,1], and JIŘÍ SEJKORA[2,3]

[1] Laboratorium für chemische und mineralogische Kristallographie, Universität Bern, Freiestrasse 3, CH-3012 Bern, Switzerland, e-mail: thomas.armbruster@krist.unibe.ch
[2] Geological Institute, University of Copenhagen, Øster Volgade 10, DK-1350 Copenhagen, Denmark
[3] National Museum, Department of Mineralogy and Petrology, Václavské nám. 68, CZ-11579 Praha 1, Czech Republic

Abstract: The crystal structure of diaphorite, $Pb_2Ag_3Sb_3S_8$, from hydrothermal veins at Příbram in central Bohemia (Czech Republic) was solved and refined from X-ray data of a crystal twinned by pseudo-merohedry. Diaphorite is monoclinic, space group $P2_1/c$, $a = 17.852(4)$, $b = 5.887(1)$, $c = 15.809(3)$ A and $\beta = 116.17(3)°$, $Z = 4$, $\varrho = 6.06$ g/cm^3. The structure can be derived from the one of galena, PbS, by the substitution $Ag^+ + Sb^{3+} \leftrightarrow 2\,Pb^{2+}$. In addition to eight S, three Sb, two Ag, and one Pb positions, the average structure exhibits also two mixed (Pb^{2+}, Ag^+) sites (M1, M2). The different coordination requirements for Pb^{2+} and Ag^+ make a complete miscibility between these ions rather unlikely. The observed structure is a family or superposition structure and four possible, maximally Pb^{2+}, Ag^+ ordered structures can be derived with space-group symmetries (1a): $P\bar{1}$, (1b) and (2a): $P2_1/n$, and (2b): $P2_1$. The structures (1a) and (2b) have the same cell dimensions as the family structure whereas structures (1b) and (2a) have a doubled **a** periodicity compared to the family structure. In addition, each of the above space groups gives rise to two different configurational variants depending on the spatial relation of homoionic occupied M1 and M2 sites.

Key-words: diaphorite, crystal structure, cation order, Pb-Ag-Sb-sulfosalt, polytypism.

Introduction

Diaphorite was described by Zepharovich (1871) as a monoclinic dimorph of orthorhombic freieslebenite. This concept was overturned by Palache *et al.* (1938) who defined diaphorite as $Pb_2Ag_3Sb_3S_8$ whereas freieslebenite as $Pb_3Ag_5Sb_5S_{12}$. Hellner (1958) determined the correct space group ($P2_1/c$; transformed to standard setting) and cell dimensions of diaphorite and derived a simplified structure model from the PbS (galena) structure type. In this model of composition $Pb_2Ag_3Sb_3S_8$ all cations occupy ideal octahedral positions within a cubic-closest packing of S atoms. However, Pb, Ag, and Sb sites were not distinguished and the characteristic distortions of their coordination polyhedra were thus not implemented in the model. Wernick (1960), studying the system PbS-$AgSbS_2$, found for the composition $Pb_2Ag_3Sb_3S_8$ above ca. 300°C what he called a β-phase of cubic symmetry with $a = 5.74$ A representing a galena-like structure with disordered (Pb, Ag, Sb) on octahedral sites. Annealing of this β-phase for 17 days at 150°C led to a product displaying a diffuse X-ray powder pattern that was different from the one of diaphorite.

Controversial interpretations of relevant, especially older chemical analyses of diaphorite continued, so that even in 1972 Sveshnikova & Borodayev found it worthwhile to revise the problem again, defining diaphorite as $Pb_2Ag_3Sb_3S_8$ but freieslebenite as $PbAgSbS_3$. Hoffman *et al.* (1977) confirmed the formula $Pb_2Ag_3Sb_3S_8$ for diaphorite from Kutná Hora, Czech Republic. Based on electron-microprobe analyses Mozgova *et al.* (1989) established a continuous compositional series between diaphorite and brongniartite on samples from various ore deposits. The substitution is $Ag^+ + Sb^{3+} \leftrightarrow 2\,Pb^{2+}$ and (Ag, Sb)-rich compositions were named brongniartite by them; they reached the composition $Pb_{1.6}Ag_{3.2}Sb_{3.2}S_8$ with similar cell dimensions as diaphorite.

The hydrothermal veins at Příbram in central Bohemia (Czech Republic) played a substantial role in the complicated history of diaphorite. It was the material from Příbram which led to the definition of diaphorite (Zepharovich, 1871) and subsequently to the clarification of its chemical composition (Palache *et al.*, 1938). The Ag-Pb-Zn hydrothermal vein deposit at Příbram is also the original locality of the sample from the collections of the National Museum, Prague, Czech Republic, examined in the present study. Associated minerals are: galena (with only 0.07 wt. % Ag), freieslebenite, and an insufficiently analysed Pb-Sb-Ag-S phase (owyheeite or zoubekite), as well as siderite. The aim of the present crystallographic study is a contribution to the understanding of Pb, Ag, Sb order and coordination distortions in sulfosalts derived from PbS.

0935-1221/03/0015-0137 $ 4.50
DOI: 10.1127/0935-1221/2003/0015-0137

Experimental

Chemical composition

Quantitative chemical analyses were carried out by means of JEOL Superprobe 733 in wavelength-dispersive mode (acceleration potential 20 kV, sample current 20 nA and 1–2 μm electron-beam diameter) with an on-line ZAF correction program supplied by JEOL. The standards and wavelengths used were: chalcopyrite [Ivigtut] (Fe$K\alpha$, S$K\alpha$, Cu$K\alpha$), synthetic Ag (Ag$L\alpha$), synthetic ZnS (Zn$K\alpha$), synthetic Sb (Sb$L\alpha$), synthetic Cu_3AsS_4 (As$L\alpha$), synthetic PbS (Pb$M\alpha$), synthetic Mn (Mn$K\alpha$) and synthetic Bi (Bi$L\alpha$). Detection limits for all ten elements were close to 0.01 wt.%. Zn, Fe and Mn were not detected.

Chemical compositions of several homogeneous diaphorite crystals from Příbram (13 point analyses) yielded the empirical formula $Pb_{1.97}Ag_{2.96}(Sb_{3.03}As_{0.01}Bi_{0.01})_{\Sigma 3.05}S_{8.02}$ calculated on the basis of 16 atoms. This composition is close to the ideal formula $Pb_2Ag_3Sb_3S_8$ (Table 1) and the structure-derived formula $Pb_{1.89}Ag_{3.11}Sb_3S_8$ (see Table 3). Minor contents of Cu are sporadic (3 analyses); traces of As and Bi were determined in about half the analyses. Minor Cu, As, and Bi concentrations in diaphorite samples from different localities were also described by Mozgova *et al.* (1989) and Frizzo & Simone (1995).

Structure determination

Single-crystal X-ray data collection on a (101) platy, elongated parallel to b, black crystal fragment of diaphorite, about 0.16 x 0.09 x 0.02 mm^3 in size, was performed with an ENRAF NONIUS CAD4 single-crystal X-ray diffractometer using graphite monochromated Mo$K\alpha$ radiation. Cell dimensions were refined from the setting angles of 20 reflections with $20° < \Theta < 29°$ yielding monoclinic symmetry with a = 17.852 (4), b = 5.887 (1), c = 15.809 (3) A and β = 116.17 (3)° (Table 2). Experimental details are given in Table 2. Diffraction data were collected up to Θ = 30°, yielding 8933 reflections of which 4336 were unique and 3512 had $F_o > 4\sigma(F_o)$ used for structure solution and refinement. Data reduction, including background and Lorentz polarization correction, was carried out with the SDP program system (Enraf Nonius, 1983). An empirical absorption correction using the ψ-scan technique was applied. Systematic absences indicated $P2_1/c$ as the only possible space group, consistent with the monoclinic symmetry of the lattice and intensity statistics ($|E^2-1| = 0.946$; expected 0.968 for centrosymmetric, 0.736 for non-centrosymmetric). The structure was solved by direct methods with the program SHELXS-97 (Sheldrick, 1997). Subsequent refinement cycles with neutral atom-scattering factors (program SHELXL-97 by Sheldrick, 1997) were accompanied by difference Fourier maps yielding eight cation and eight sulfur positions. Cation assignment was based on interatomic distances and scattering power. Refinement of individual site occupancies indicated cation substitution for two sites with Ag:Pb ratios of about 50:50 (Table 3). Anisotropic displacement parameters were refined for all atoms in the last cycles. The highest residual peak was 2.73 e/ A^3, 0.82 A from Pb1 and the deepest hole -3.38 e/ A^3, 0.98 A from M1 at the end of the refinement. The refinement was stopped when the maximum shift/esd for varied parameters dropped below 0.01. The refinement results are represented in Tables 3, 4, 5, and 6.

Table 1. Chemical composition of diaphorite from Příbram.

	Příbram			Theor.
	mean (wt.%)	range (wt.%)	[1]	[2]
Ag	23.46	23.00–23.82	2.964	23.87
Cu	0.02	0–0.08	0	–
Pb	29.93	29.25–30.48	1.968	30.48
Sb	27.1	26.89–27.34	3.033	26.87
As	0.05	0–0.11	0.01	–
Bi	0.07	0–0.27	0.01	–
S	18.86	18.44–19.17	8.017	18.87
total	99.49			100

[1] molar ratio on the basis of 16 atoms

[2] theoretical composition of $Pb_2Ag_3Sb_3S_8$ in wt.%

Table 2. Summarized data collection and structure refinement parameters for diaphorite.

Diffractometer	Enraf Nonius CAD4
X-ray radiation	Mo$K\alpha$
X-ray power	50 kV, 40 mA
Temperature	293 K
Space group	$P2_1/c$
cell dimensions (A, °)	
a	17.8520(36)
b	5.8870(12)
c	15.8090(32)
β	116.165(30)
Maximum 2 Θ	59.95°
Measured reflections	8933
Index range	$0 \le h \le 25$, $-8 \le k \le 8$, $22 \le l \le 19$
Observed reflections	8933
Unique reflections	4336
Reflections > $2\sigma(I)$	3512
R_σ	3.23%
Number of l.s. parameters	149
GooF	1.047
R_1, $F_o > 4\sigma(F_o)$	4.18%
R_1, all data	5.65%
wR_2 (on F_o^2)	11.82%

$R_{int} = \Sigma\, |F_o^2 - F_o^2\,(\text{mean})| \,/\, \Sigma\, F_o^2$

$R_\sigma = \Sigma\, \sigma(F_o^2) \,/\, \Sigma\, F_o^2$

$R_1 = \Sigma\, ||F_o| - |F_c|| \,/\, \Sigma\, |F_o|$

$wR_2 = \sqrt{(\Sigma\, w[F_o^2 - F_c^2]^2 \,/\, \Sigma\, w[F_o^2]^2)}$

$\text{Goof} = \sqrt{(\Sigma\, w[F_o^2 - F_c^2] \,/\, [n\text{-}p])}$

$w = 1 \,/\, (\sigma^2[F_o^2] + [0.0712 * P]^2 + 7.18 * P)$

$P = (\text{Max}\,[F_o^2, 0] + 2 * F_c^2) \,/\, 3$

Table 3. Fractional atomic coordinates and isotropic displacement parameters for diaphorite, with estimated standard deviations in parentheses.

Atom	Occupancy	*x/a*	*y/b*	*z/c*	U_{iso}
Pb1	1	0.18973(2)	-0.31003(7)	0.54127(3)	0.02062(12)
M1	0.516(5) Ag 0.484(5) Pb	0.06451(4)	0.19426(11)	0.34402(4)	0.0274(2)
M2	0.596(5) Ag 0.404(5) Pb	0.30967(4)	0.28176(14)	0.22247(4)	0.0302(2)
Ag3	1	0.43323(8)	0.7581(3)	0.14479(9)	0.0436(3)
Ag4	1	0.19471(8)	0.7117(2)	0.28096(8)	0.0488(3)
Sb1	1	0.31616(4)	0.21030(11)	0.46489(5)	0.01691(15)
Sb2	1	0.43998(4)	0.76228(13)	0.39980(5)	0.01630(15)
Sb3	1	-0.06306(4)	-0.28248(11)	0.39950(5)	0.01611(15)
S1	1	0.21050(18)	0.1518(4)	0.5268(2)	0.0258(6)
S2	1	-0.07340(19)	0.1276(4)	0.3823(2)	0.0248(5)
S3	1	0.29638(16)	0.6251(4)	0.45152(18)	0.0171(4)
S4	1	0.17373(18)	0.1536(6)	0.2598(2)	0.0291(6)
S5	1	0.44417(18)	0.3501(4)	0.3896(2)	0.0235(5)
S6	1	0.05450(16)	0.6754(5)	0.35830(19)	0.0203(5)
S7	1	0.34461(17)	0.8159(5)	0.23088(17)	0.0223(5)
S8	1	0.43137(15)	0.1945(4)	0.62829(18)	0.0189(5)

Table 4. Anisotropic displacement parameters for diaphorite, with estimated standard deviations in parentheses.

Atom	U_{11}	U_{22}	U_{33}	U_{23}	U_{13}	U_{12}
Pb1	0.0184(2)	0.0194(2)	0.0237(2)	0.00138(14)	0.00901(16)	0.00031(14)
M1	0.0241(3)	0.0305(4)	0.0302(4)	0.0019(2)	0.0144(3)	-0.0002(2)
M2	0.0282(4)	0.0349(4)	0.0190(3)	0.0012(3)	0.0027(3)	-0.0021(3)
Ag3	0.0519(7)	0.0362(5)	0.0634(8)	0.0001(6)	0.0443(7)	-0.0028(5)
Ag4	0.0519(7)	0.0411(7)	0.0298(5)	0.0039(5)	-0.0035(5)	-0.0007(6)
Sb1	0.0150(3)	0.0146(3)	0.0200(3)	-0.0011(2)	0.0066(3)	-0.0001(2)
Sb2	0.0159(3)	0.0147(3)	0.0180(3)	-0.0005(3)	0.0072(3)	0.0007(2)
Sb3	0.0151(3)	0.0157(3)	0.0174(3)	0.0022(2)	0.0070(3)	0.0007(2)
S1	0.0274(14)	0.0165(11)	0.0451(16)	0.0014(11)	0.0266(13)	0.0004(10)
S2	0.0317(14)	0.0181(11)	0.0264(13)	0.0010(10)	0.0145(12)	0.0037(10)
S3	0.0167(11)	0.0148(10)	0.0202(11)	0.0002(9)	0.0085(9)	0.0000(9)
S4	0.0204(13)	0.0308(14)	0.0246(13)	0.0012(11)	-0.0006(11)	0.0034(11)
S5	0.0301(14)	0.0150(11)	0.0332(14)	-0.0001(10)	0.0210(12)	-0.0001(10)
S6	0.0144(11)	0.0256(13)	0.0207(11)	-0.0015(10)	0.0077(9)	0.0003(10)
S7	0.0183(11)	0.0277(13)	0.0162(11)	0.0014(10)	0.0031(9)	0.0028(10)
S8	0.0129(11)	0.0228(13)	0.0187(11)	0.0028(9)	0.0050(9)	-0.0005(9)

The investigated crystal displayed pseudo-merohedral twinning (Herbst-Irmer & Sheldrick, 1998) according to the twin law $\mathbf{R} = (101, 010, 00\bar{1})$ converging to a twin domain ratio of about 9:1. Without consideration of this twinning $R_1 = 8.33$ % and $wR_2 = 25.76$ % were about twice as high as after the twin refinement. In addition, neglecting the twinning leads to increased (by a factor of three) esd's of bond lengths. Another warning for twinning (Herbst-Irmer & Sheldrick 1998) comes from the variance analysis of reflections using the grouped K statistics where $K = \text{Mean}[F_o^2]/\text{Mean}[F_c^2]$. The group with $F_c/F_c(\text{max})$ between 0.00 and 0.013 (the 500 weakest reflections) yielded $K = 4.255$ and is thus strongly deviating from the ideal K value of 1. After introduction of twinning K decreased to 1.326. The pseudo-merohedral twinning is related to the existence of higher metric symmetry as evidenced by a *C*-centred pseudo-orthorhombic cell of $a = 15.809$, $b = 32.045$, $c = 5.887$ A, $\gamma = 89.88°$ (*e.g.*, Hellner, 1958).

Structure description

The crystal structure of diaphorite is a PbS-based structure type with partial substitution of the cations by Ag and Sb. The diaphorite structure contains one Pb site, two mixed (Pb,Ag) sites, two Ag sites, three distinct Sb sites and eight S positions. All of them are in the general Wyckoff position 4e of the space group $P2_1/c$; no special positions are occupied. All cations have six close ligands which form distorted octahedra.

Polygonal (010) sheets

Description of the diaphorite structure by means of (010) sheets of atoms is the best means of introduction to its 3-D analysis. However, it ignores the upward and downward orientation of individual Sb polyhedra, resulting in a halved

Table 5. Selected interatomic distances [A] and angles [°] for diaphorite, with estimated standard deviations in parentheses.

Pb1	S1	S6	S3	S2	S7	S1
S1	2.767(3)	91.7(1)	87.0(1)	79.9(1)	89.8(1)	160.1(1)
S6	4.022(4)	2.836(2)	86.8(1)	89.6(1)	174.9(1)	88.3(1)
S3	3.872(4)	3.911(4)	2.858(3)	166.3(1)	88.4(1)	73.1(1)
S2	3.723(5)	4.130(5)	5.839(5)	3.023(4)	95.5(1)	120.0(1)
S7	4.112(4)	5.884(3)	4.125(4)	4.498(4)	3.053(2)	88.6(1)
S1	5.887(4)	4.220(4)	3.625(4)	5.399(4)	4.376(4)	3.210(3)
M1	S2	S4	S6	S1	S6	S6
S2	2.810(4)	161.0(1)	91.7(1)	105.0(1)	87.0(1)	76.1(1)
S4	5.547(6)	2.814(4)	101.7(1)	87.6(1)	78.6(1)	91.4(1)
S6	4.065(4)	4.395(5)	2.853(3)	93.8(1)	94.7(1)	166.6(1)
S1	4.552(4)	3.976(5)	4.220(4)	2.926(2)	165.0(1)	84.1(1)
S6	3.974(5)	3.660(4)	4.278(4)	5.837(3)	2.960(3)	90.3(1)
S6	3.634(4)	4.219(5)	5.887(4)	4.022(4)	4.278(4)	3.074(3)
M2	S5	S7	S1	S4	S8	S7
S5	2.704(2)	90.9(1)	154.7(1)	108.0(1)	87.4(1)	74.9(1)
S7	3.926(4)	2.803(3)	101.9(1)	85.6(1)	83.1(1)	157.7(1)
S1	5.404(4)	4.376(4)	2.833(3)	94.8(1)	72.9(1)	85.8(1)
S4	4.486(4)	3.834(5)	4.177(5)	2.841(4)	161.1(1)	114.9(1)
S8	4.044(5)	3.944(4)	3.551(4)	5.891(5)	3.132(3)	79.2(1)
S7	3.611(4)	5.887(4)	4.112(4)	5.094(5)	4.034(4)	3.197(3)
Ag3	S7	S5	S8	S3	S8	S8
S7	2.524(4)	153.2(1)	101.7(1)	95.4(1)	85.6(1)	74.8(1)
S5	4.921(5)	2.535(4)	99.6(1)	97.1(1)	75.5(1)	85.9(1)
S8	4.034(4)	3.981(4)	2.676(3)	99.1(1)	170.3(1)	99.2(1)
S3	4.125(4)	4.186(4)	4.349(3)	3.032(3)	73.6(1)	160.7(1)
S8	3.944(4)	3.572(4)	5.887(4)	3.756(3)	3.232(3)	88.9(1)
S8	3.620(4)	4.044(5)	4.600(3)	6.281(3)	4.600(3)	3.338(3)
Ag4	S3	S2	S4	S7	S6	S4
S3	2.551(3)	155.6(1)	109.1(1)	91.0(1)	84.0(1)	84.5(1)
S2	5.017(3)	2.582(3)	93.0(1)	102.5(1)	85.3(1)	72.6(1)
S4	4.220(4)	3.781(4)	2.629(4)	82.3(1)	91.3(1)	165.2(1)
S7	4.101(5)	4.498(4)	3.834(5)	3.167(4)	170.1(1)	103.7(1)
S6	3.911(4)	3.974(5)	4.219(5)	6.385(5)	3.241(4)	84.3(1)
S4	3.979(4)	3.535(4)	5.887(5)	5.094(5)	4.395(5)	3.307(4)
Sb1	S3	S8	S1	S5	S4	S3
S3	2.463(3)	98.5(1)	93.8(1)	78.9(1)	89.8(1)	167.2(1)
S8	3.756(3)	2.495(2)	90.5(1)	89.8(1)	171.7(1)	92.4(1)
S1	3.625(4)	3.551(4)	2.502(4)	172.6(1)	89.0(1)	79.2(1)
S5	3.580(5)	3.986(5)	5.608(5)	3.117(4)	91.7(1)	108.2(1)
S4	3.979(4)	5.615(3)	3.976(5)	4.486(4)	3.134(3)	79.4(1)
S3	5.887(4)	4.349(3)	3.872(4)	5.330(4)	4.220(4)	3.460(3)
Sb2	S5	S7	S8	S5	S3	S5
S5	2.435(3)	94.7(1)	91.8(1)	80.4(1)	79.2(1)	171.8(1)
S7	3.611(4)	2.474(2)	92.5(1)	175.0(1)	93.6(1)	80.9(1)
S8	3.572(4)	3.620(4)	2.537(3)	89.0(1)	169.5(1)	81.5(1)
S5	3.625(4)	5.588(4)	3.986(5)	3.119(3)	84.3(1)	104.1(1)
S3	3.580(5)	4.101(5)	5.635(5)	4.186(4)	3.121(3)	107.9(1)
S5	5.887(4)	3.926(4)	3.981(4)	5.198(4)	5.330(4)	3.467(3)
Sb3	S2	S4	S6	S2	S1	S2
S2	2.427(3)	92.9(1)	95.8(1)	80.2(1)	77.4(1)	169.9(1)
S4	3.535(4)	2.449(3)	96.2(1)	171.8(1)	89.5(1)	77.0(1)
S6	3.634(4)	3.660(4)	2.469(4)	89.0(1)	171.4(1)	84.3(1)
S2	3.791(4)	5.790(4)	4.130(5)	3.355(3)	84.7(1)	109.9(1)
S1	3.723(5)	4.177(5)	5.856(5)	4.552(4)	3.403(4)	103.3(1)
S2	5.887(4)	3.781(4)	4.065(4)	5.598(4)	5.399(4)	3.482(3)

Table 6. Principal mean square atomic displacements <*U*> in [A^2].

Pb1	0.0245	0.0190	0.0183
M1	0.0322	0.0289	0.0211
M2	0.0405	0.0331	0.0170
Ag3	0.0717	0.0367	0.0224
Ag4	0.0824	0.0412	0.0228
Sb1	0.0213	0.0150	0.0144
Sb2	0.0185	0.0162	0.0142
Sb3	0.0191	0.0151	0.0142
S1	0.0470	0.0166	0.0138
S2	0.0327	0.0246	0.0171
S3	0.0202	0.0162	0.0148
S4	0.0418	0.0310	0.0144
S5	0.0367	0.0189	0.0150
S6	0.0263	0.0205	0.0140
S7	0.0288	0.0247	0.0136
S8	0.0254	0.0184	0.0128

c period. Moreover, the monoclinic angle β is a direct consequence of the sequences with upward and downward orientation in the adjacent [010] ribbons of polyhedra.

The **pseudotetragonal (010) subnet** of diaphorite (Hellner, 1958) is distorted by coordination requirements of Pb, Ag, and Sb of the types commonly observed in sulfosalts. The resulting modified (010) sheet can be described as composed of three kinds of [001] stripes (Fig. 1):

(a) Square coordination polygon of $Pb1S_4$ (formed by S2, S3, S6, and S7), and a coordination lozenge of $Ag4S_4$ (formed by S2, S3, S6, and S7) build zig-zag stripes repeating in the (010) sheet with periodicity $\vec{d}$ (100).

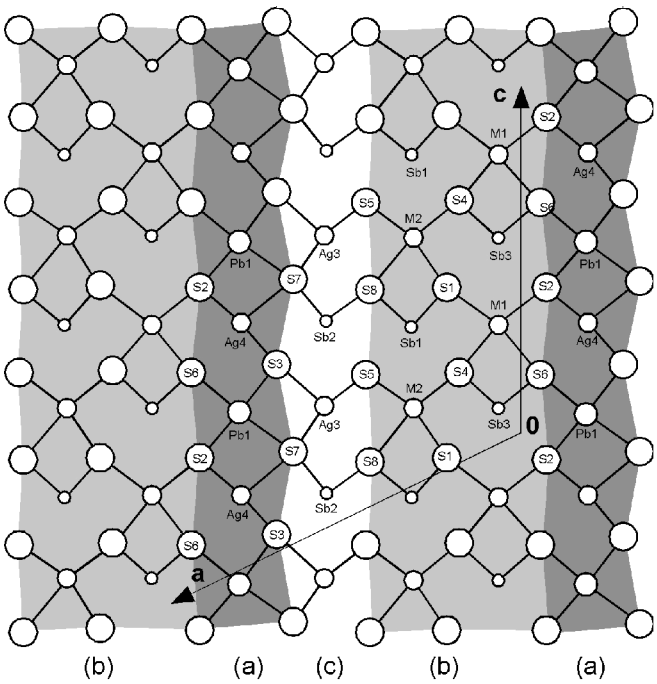

Fig. 1. The unit (010) net at y≈$^1/_4$ form the crystal structure of diaphorite. In order of decreasing size, circles indicate S, Pb, mixed positions, Ag, and Sb. Only short cation-sulfur distances are indicated. The three kinds of unit stripes, (a) – (c), are discussed in the text.

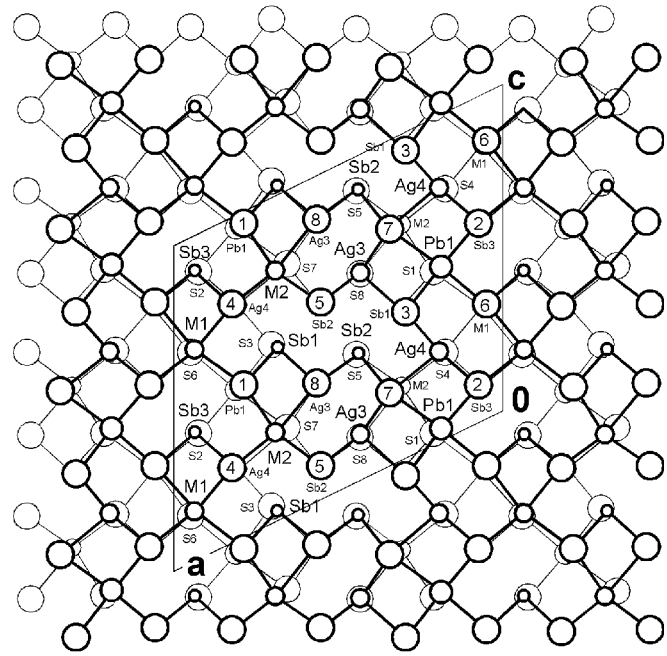

Fig. 2. The crystal structure of diaphorite presented as two adjacent nets. Different label sizes indicate atoms in the upper and lower net, at y=$^1/_4$ and $^3/_4$, respectively. Labels of sulfur atoms in the upper net are given as simple numerals. Only short Sb-S and Ag-S distances are indicated.

(b) A double stripe of Sb1-centred (S1, S4, S5, S8) and Sb3-centred (S1, S2, S4, S6) trapezoids alternating with trapezoids of mixed (Ag, Pb) positions centred by M1 (S1, S2, S4, S6) and M2 (S1, S4, S5, S8) flanks the (a) stripe on one side; its internal configuration is based on a glide plane parallel to (100).

(c) A stripe of Sb2-centred trapezoids (S3, S5, S7, S8) alternating with Ag3-centred lozenges (S3, S5, S7, S8) is attached to the opposing side of the (a) stripe, with the Ag3 lozenges edge-sharing with the Pb1 squares and the Sb2 trapezoids joining the Ag4 lozenges.

The latter Ag3-Sb2 sequence is approximately reflected by a (100) mirror plane passing through S5 and S8 onto the M2 and Sb1 sequence from (b), forming visually conspicuous pairs of Sb1 and Sb2 coordination pyramids (actually formed by S1, S4, S5, S8 (S3, S5, S7 S8) as basis and S3 (S5) of the shorter Sb1-S3 (Sb2-S5) bond as apex), situated about the x ≈ 0.43 plane. The adjacent upper and lower (010) sheets are related to the original sheet by a 2_1 operation at 0, ¼ and ½, ¼, completing the coordination polyhedra of cations.

Coordination polyhedra

The slightly trapezoidal **coordination octahedron of Pb1** displays two shorter bonds, 2.836 and 2.858 A in the (010) plane, opposed by longer distances equal to 3.053 and 3.023 A (Fig. 3). Asymmetry is substantially larger in the [010] direction, the corresponding Pb1-S1 distances being 2.767 and 3.210 A. Considering the distances observed in Pb-Sb

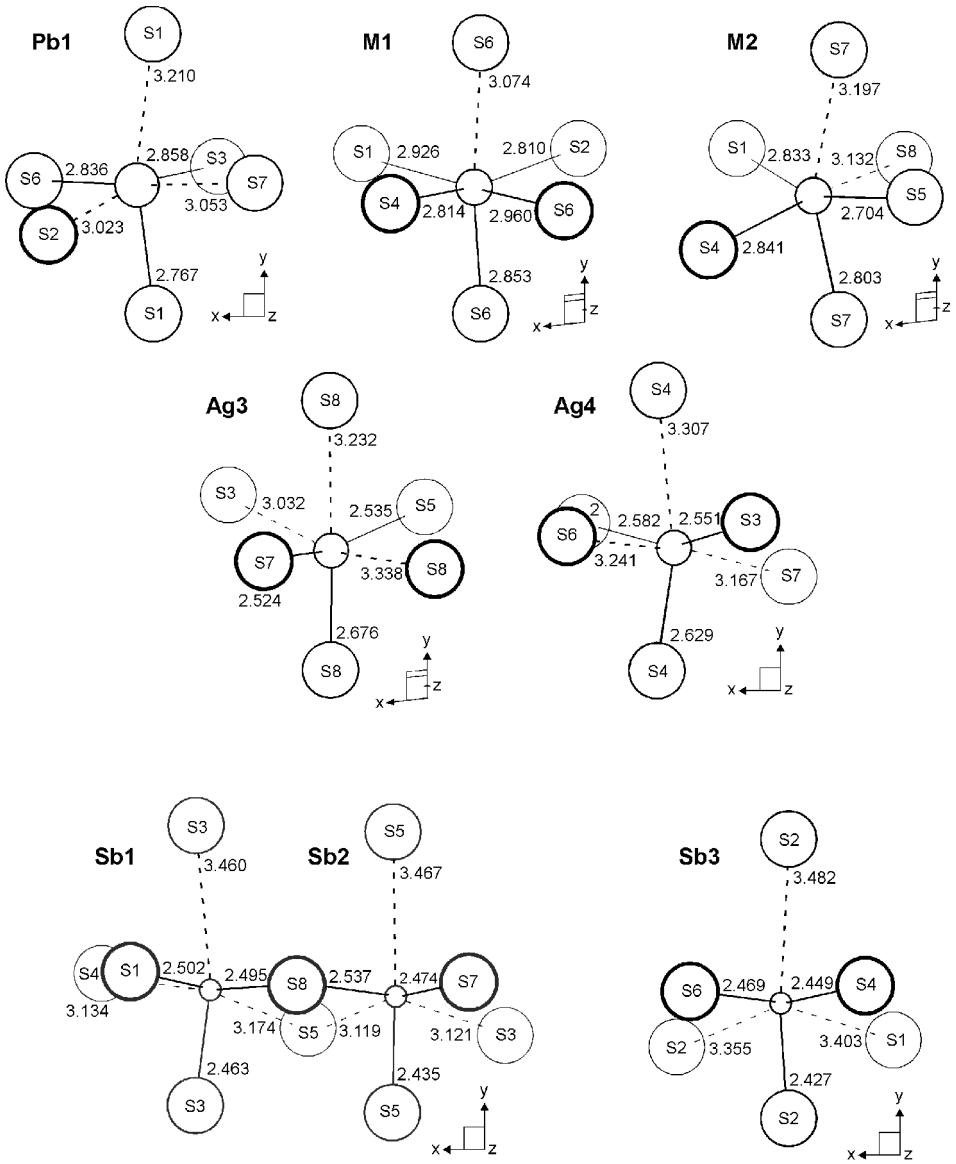

Fig. 3. Coordination polyhedra of the cations in the structure of diaphorite. Distances are given in A.

sulfosalts with simple composition, such as freieslebenite $PbAgSbS_3$ (Ito & Nowacki, 1974), with the full range of Pb-S distances being 2.806–3.167 A, we find the Pb1 site in diaphorite somewhat stressed, probably owing to the decrease in unit-cell dimensions due to the advanced Ag-Sb substitution. The octahedral coordination of Pb1 with a warped trapezoidal base is similar to freieslebenite, but the vertical asymmetry in the latter is less pronounced: 2.892 *vs.* 3.102 A.

The **Ag3 and Ag4 sites** have coordination octahedra with a lozenge-like cross-section in the (010) plane, with an essentially linear two-fold coordination (a range 2.524 to 2.582 A, Fig. 3, Table 5) that is supplemented by a slightly longer bond, 2.676 and 2.629 A, respectively, for the two Ag sites. This bond extends to an S atom lying above or below the Ag site in the [010] direction. The Ag atom is visibly displaced from the linear configuration towards this third short-bonded S atom: the angle of the quasi-linear bond is 153.2° and 155.6°, respectively, instead of 180°. The $Ag3S_3$ group is only slightly non-planar, the sum of bond angles being 354.5°; the $Ag4S_3$ group (Fig. 3) is almost planar (sum of 357.7°).

The similarity of this arrangement to the bonding scheme of Ag in freieslebenite (Ito & Nowacki, 1974) – 2.522, 2.575, 2.687 and 2.928 A – and in smithite (Hellner & Burzlaff, 1964) – Ag1: 2.51, 2.56, 2.68, and 2.84 A; Ag2: 2.52, 2.55, 2.65, and 2.90 A – suggests a configurational rigidity of this scheme. The third shortest bond (2.687 A) in freieslebenite is oriented perpendicular to the plane of the coordination lozenge, as is in diaphorite. However, in diaphorite the distances to the fourth S atom (3.032 and 3.167 A, respectively) are longer than in the quoted examples.

Both Ag sites have highly anisotropic displacement parameters; the displacement ellipsoid is perpendicular to the plane of the triangle formed by the three shortest bonds. In Ag3 it roughly points along the [102] direction, whereas in Ag4 along the $[20\bar{1}]$ direction.

The solitary **Sb3 site** has a slightly distorted "Sb-like" coordination of three short bonds (2.427, 2.449, and 2.469 A, bond angles 92.9–96.2°), opposed by much longer Sb-S distances (3.355, 3.403, and 3.482 A), revealing an active and symmetrically placed lone electron pair. The 2.427 A bond is perpendicular to the (010) plane and is counterbalanced by the distance of 3.482 A. Two Sb3 atoms placed next to each other around an [010] line (Fig. 2) have the 2.427 A bonds oriented in the opposite directions, creating a small, two-atom lone electron pair micelle and fragments of tightly-bonded atomic double-layers (groups of two SbS_5 pyramids sharing an inclined edge) between them. These fragments and micelles alternate along the [010] direction.

The **Sb1-Sb2 pairs** (Fig. 2) on the one hand form, together with symmetry-related Sb1-Sb2 groups of pyramids, large lone-electron pair micelles extended parallel to $\vec{d}_{100}$ and on the other, groups of four edge-sharing Sb pyramids with bases parallel to (010). These two elements are interleaved in the [010] direction, the latter of them forms a distorted PbS like motif surrounded by other coordination polyhedra.

The patterns of the three shortest distances are more distorted than for Sb3; the distances to the common S8 atom are 2.495–2.537 A; those to free pyramidal vertices are shortest, 2.463 and 2.435 A, respectively, backed by the longest ones (3.460 and 3.467 A across the micelle). The longer Sb1-S1 bond, 2.502 A, connects the corners of Sb1 and Sb3 pyramids, continuing as the S1-Sb3 distance of 3.403 A, the second longest distance in this polyhedron.

The two **mixed-cation sites (M1, M2)** differ in their position and coordination. M1 has an octahedral coordination with a trapezoidal cross-section; it alternates with Sb3 along the [001] direction. The octahedron of M2 is "half-trapezoidal", abutting the lozenge of Ag3; these two polyhedra are alternating with the Sb1-Sb2 pair. These mixed cation positions were refined as mixed sites Ag and Pb, in which the Pb fraction is 0.483 and 0.404, for M1 and M2, respectively. Maximum principal mean-square atomic displacements for them are augmented in comparison with Pb1 and Sb1-Sb3 but are still less than a half of those for pure Ag (Table 6).

The bond distances (Table 5) have a mixed character: the angles between the three shortest distances remind us of Ag and not Pb but their lengths and distribution are more Pb-like, exceeding by far the shortest Ag-S distances. The sulfur atoms with the highest displacement factors (Tables 3 and 4) are (1) S1 that participates in both the M1 and the M2 polyhedron, (2) S2 that forms the shortest bond in the M1 polyhedron, (3) S5 ditto in M2 and (4) S4, again participating in both polyhedra.

Polyhedron-distortion parameters

In the process of characterization of polyhedron distortion (Balić-Žunić & Makovicky, 1996; Makovicky & Balić-Žunić, 1998), a least-squares-fitted sphere is circumscribed to the coordination polyhedron. Its volume (V_s) is compared to that of the polyhedron examined (V_p) and to the volume of an ideal polyhedron (V_i) with the same coordination number (CN), which is inscribed in the same sphere as the observed polyhedron. This comparison yields a measure of polyhedron distortion (υ). 'Sphericity' (SPH_v) is a measure of the fit of ligands to the sphere, and 'eccentricity' (ECC_v) expresses a displacement (Δ) of the cation from the centre of the sphere (explanations are introduced as a footnote to Table 7). All calculations have been performed for CN = 6.

Table 7 shows that, in terms of SPH_v, the most symmetric polyhedra are those of Pb1 and Sb3, which also are the largest polyhedra with CN = 6 in the structure whereas those of Ag3, Ag4 and M2 are most distorted. Pb1 and the mixed positions (M1, M2) are placed fairly centrally in their polyhe-

Table 7. Polyhedron distortion parameters for cations in diaphorite.

Atom	CN	$r_s(\sigma[r_s])$	V_s	V_p	υ	Δ	BC	ECC_v	SPH_v
Pb1	6	2.987(27)	111.626	32.631	0.0816	0.29	0.44	0.2625	0.9733
M1	6	2.901(79)	102.307	31.722	0.0259	0.11	0.13	0.1046	0.9186
M2	6	2.908(137)	102.966	30.869	0.0581	0.22	0.28	0.2095	0.8589
Ag3	6	2.866(312)	98.627	30.211	0.0377	0.31	0.13	0.2915	0.673
Ag4	6	2.910(321)	103.204	31.132	0.0523	0.27	0.17	0.2493	0.6685
Sb1	6	2.925(68)	104.842	30.186	0.0955	0.72	0.53	0.5735	0.9303
Sb2	6	2.967(63)	109.355	29.870	0.1419	0.78	0.70	0.5994	0.9361
Sb3	6	3.081(32)	122.477	31.921	0.1812	0.99	0.84	0.6853	0.9687

Notes: The centroid parameters used are defined in Balić-Žunić & Makovicky (1996) and Makovicky & Balić-Žunić (1998). The volume distortions (υ) are calculated using the maximum volume polyhedon for CN = 6 (octahedron)

CN coordination number

r_s radius of the sphere fitted by least squares to the ligands of distinct coordination polyhedra and its standard deviation $\sigma(r_s)$

V_s sphere volume

V_p polyhedron volume

υ Volume distortion $\upsilon = (V_i - V_p) / V_i$ to be multiplied by 100 to obtain percentage

Δ The distance AC from the central atom (A) to the centroid (= sphere centre, C)

BC The distance from the central atom (A) to the barycentre (B)

ECC_v "volume-based" eccentricity $ECC_v = 1-[(r_s-\Delta)/r_s]^3$ where r_s is the radius of the circumscribed sphere and Δ is the distance between the sphere centre ('centroid') and the central atom

SPH_v "volume-based" sphericity $SPH_v = 1–3\sigma_r/r_s$ where σ_r is a standard deviation of the radius r_s

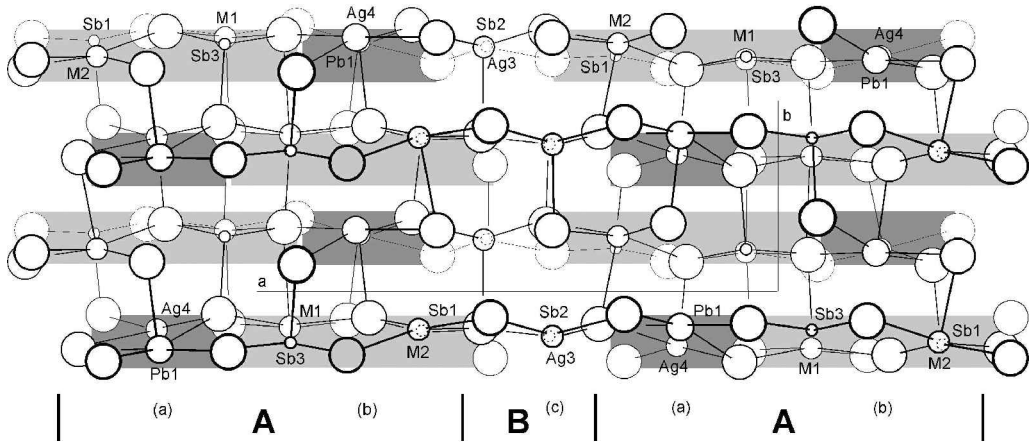

Fig. 4. The crystal structure of diaphorite projected along [001]. Stripes (a) are dark grey, stripes (b) are light grey, and stripes (c) are white. Stripe types and idealized boundaries of OD layers A and B are indicated below the figure (see text for details).

dra, the cation – centroid (sphere centre) distance Δ, respectively, being 0.29, 0.11 and 0.22 A. Ag atoms are on average more eccentric (0.31 and 0.27 A, respectively, for Ag3 and Ag4), whereas the Sb atoms are very eccentric (0.72, 0.78 and 0.99 A for Sb1-Sb3); the latter eccentricity expresses the active role of the lone electron pair in filling the octahedral space allotted to Sb.

The role and spatial distribution of short and long cation-ligand distances in shaping the cation polyhedron can also be expressed comparing the position of the barycentre of all ligands with that of the centroid. In the above cation sequence, the distance (barycentre – centroid) is 0.44, 0.13, 0.28 A for Pb1, M1 and M2, 0.13 and 0.17 A for Ag3 and Ag4 but it is 0.53, 0.70 and 0.84 A for Sb1, 2 and 3. These data corroborate the symmetrical distribution of ligands at highly differing distances in the case of Ag (and Ag-containing positions) and the accumulation of ligands on one side of the coordination spheres of all three Sb atoms.

Polytypism and OD layers

The coordination differences between Ag and Pb make a full substitutability of these elements in a structure unlikely. Therefore, an attempt is made here to explain the mixed M1 and M2 positions by a disorder of internally ordered blocks of the structure. The observed structure would then be a **superposition structure** of diaphorite.

The most straightforward explanation of the observed diaphorite structure by order-disorder phenomena can be obtained by dividing it into two sets of alternating layers. The A layers are three polyhedra thick (100) layers, in which Ag and Pb alternate along the [001] direction in those layer portions that are based on the (b) stripes mentioned in the previous sections. The (a) stripe is interleaved with the (b) stripes in these (100) layers (Fig. 2, 4). The alternating Ag and Pb polyhedra in the (b) portions are separated by Sb1 and Sb2 polyhedra. These Ag and Pb polyhedra will be averaged in the process of random mutual shifts of adjacent A layers by *c*/2 increments along [001] and will result in the mixed metal sites (M1) and (M2). To the contrary, the mutually very similar Sb1 and Sb1', respectively Sb3 and Sb3' polyhedra which associate with the above, will average into pure Sb sites denoted as Sb1 and Sb3 of the (b) portions. For the (a) stripes incorporated in these (100) A layers, similar *c*/2 shifts lead to overlaps of the same kinds of metals and polyhedra, *e.g.*, Pb1 with Pb1' and Ag4 with Ag4', respectively.

B layers are the Sb2-Ag3 interlayers, based on pure (c) stripes. They are situated in the median (100) plane of the unit cell, straddling x = 0.5 (Fig. 4). This layer type possesses a set of 2_1 axes parallel to [010], and symmetry centres; these two sets alternate along [001]. It also has a set of *c*-glide planes parallel to (010). Thus, the B layer has layer group *P* (1) $2_1/c1$; the element in parentheses is in the direction perpendicular to this layer.

The above-defined A (100) layers are in the ordered structure related either by 2_1 or by $\bar{1}$ operators situated in the B layer. However, the B layer separates them and the two possible positions of the second A (100) layer in respect to the initial A layer are fully equivalent when related to the intervening B layer. It means that diaphorite can be described using the formalism for OD structures (Ďurovič, 1997) composed of two types of layers. We may stress the different thickness of these two OD layers: a three octahedra thick A layer composed of a combination of (a) and (b) stripes, and the B layer, one octahedron thick and composed of (c) stripes only (Fig. 4).

The A layer of the **superposition structure** has 2_1 operators, parallel to **b** and situated at x = 0, z = ¼, and symmetry centres at 0, 0, ½ and 0, ½, ½, in addition to *c* glide planes (010) in the planes of the cation sheets. If the Ag/Pb alternation is introduced into the mixed metal (M1) and (M2) positions, the 'right-' and 'left'-hand parts of the A layer will be related either by 2_1 or by $\bar{1}$ operators at x = 0. Over the entire 2_1-based zig-zag M1-M1'columns [010] of mixed-cation polyhedra in the 3D superposition structure, these two situations result in different arrangements. For the 2_1 operators pure Ag-Ag-Ag and Pb-Pb-Pb columns will result at x = 0 and z = ¼ and ¾, respectively, whereas for the $\bar{1}$ operation, combined Ag-Pb-Ag-Pb columns at x = 0 and z equal to both ¼ and ¾ will be formed. In either case, the *c* glide planes of the superposition structure are lost due to the

Ag and Pb alternation and the A layer will have layer symmetry either $P\bar{1}$ or $P2_1$.

The surfaces of the A and B layers must be drawn on those planes where two such OD layers can slide freely past one another by the *c*/2 increment. Let us examine first the stack, along [010], of alternating (a) stripes and (b) stripes (Fig. 1, 2 and 4) in the A layers. In this stack, the (a) stripe lies always above and below the median line of the stripe (b). The stack of (c) stripes in the B layers adjusts to this by a sinuous or zig-zag stacking along [010]. The resulting (100) boundary between adjacent A and B layers consists of a wavy (a)/(c), (b)/(c), *etc.* sequence of contacts when proceeding along the [010] direction.

The two alternatives, Ag-Pb-Ag-Pb and Ag-Ag-Ag & Pb-Pb-Pb, for the order of cations in the zig-zag 2_1 columns of the superposition structure in the central zone of the A (100) layers, at x = 0, represent two alternative positions of the second half of the A layer against the first half of it. The change in chemistry (and symmetry contents, *viz.*- 2_1 *versus* $\bar{1}$) of the above-mentioned zig-zag columns indicates that these two alternatives do not represent two fully equivalent positions of the second sublayer after the first one, *i.e.*, a true OD relationship between the two immediately adjacent sublayers of the A (100) layer does not exist. Although this type of polytypism cannot be fully excluded, a slab of double thickness (*i.e.*, an A layer), composed of two such (100) sublayers probably almost always forms an ordered structure with fixed Ag and Pb positions.

When modelling the structures with **maximum degree** of **order** (**MDO's**), in the absence of evidence about which of the two above alternatives (*i.e.*, the alternating zig-zag columns with one kind of cation *versus* only one kind of mixed, Ag-Pb columns) is preferred, we have to start with both these variants. As already mentioned, there are two sets of symmetry elements, those at x = 0, in the A layer and those at x = 0.5, *i.e.,* in the B layer. In what follows, the former will be left unmarked whereas the latter will be indicated by an asterisk. In order to express the Ag-Pb-Ag-Pb alternation in the zig-zag columns of originally 'mixed' cation sites, the language of dichroic symmetry will be adopted: those operations which change Ag into Pb or *vice versa*, will be primed; those which preserve the given kind of cation remain unprimed. Only unprimed elements generate systematic extinctions in the weighted reciprocal lattice.

For the case of zig-zag columns at x = 0 and z = ¼, ¾, with regularly alternating Ag and Pb atoms,

(1a) in the case of unprimed $\bar{1}$* operators in the B layer, the resulting symmetry is
$\{a, c\}\ P2'_1/c'(\bar{1})\ \{2'_1; \bar{1}\}^*$ (*i.e.*, $P\bar{1}$).

(1b) in the case of unprimed 2_1* operators in the B layer, this symmetry is
$\{2a,c\}P_{a'}2_1^*/(n;c')(\bar{1})\ \{2'_1; \bar{1}'^*\}$ (*i.e.*, $P2_1/n$).

For the case of compositionally uniform zig-zag 2_1 columns (*i.e.*, pure Ag-Ag and Pb-Pb columns),

(2a) the case with unprimed $\bar{1}$* operators in the B layer gives
$\{2a, c\}\ P_{a'}2_1/(n;c')(\bar{1}')\ \{2'_1, \bar{1}\}^*$ (*i.e.*, $P2_1/n$).

(2b) the case with unprimed 2_1* operators in the B layer gives
$\{a, c\}\ P2_1/c'(\bar{1}')\ \{2_1, \bar{1}'\}^*$ (*i.e.*, $P2_1$).

In the reciprocal space, cases 1*a* and 2*b* yield unit cells based on the same **a*** and **c*** vectors as the family structure; its *c*-glide extinction disappears, however. The cases with doubled *a* parameter will exhibit *n* glide extinctions for the *h*0*l* reflections and a halved **a*** axis. It should be noted that the bulk of changes against the family space group $P2_1/c$ will be produced by the $\Delta Z = Z_{Pb}-Z_{Ag}$ effect for 8 out of 32 metal positions, *i.e.*, by the ratio of 280 to 2344 electrons which is equal to 0.119 for $\Sigma Z = 2344$ in the formula unit $Pb_8Sb_{12}Ag_{12}S_{32}$. Therefore, a random sequence of ordered (100) slabs of variable thickness should bring about only a weak streaking parallel to **a***.

After the polytypic model of diaphorite had been worked out, the diaphorite crystal was remounted on a Siemens SMART three-circle diffractometer (Mo$K\alpha$ radiation) equipped with a CCD-based area detector. Even after an exposure time of 6 minutes per frame no indication of streaking or faint reflections indicating doubling of *a* could be found. Moreover, no reflections violating the *c* glide of the family structure have been found.

In the above scheme, we fixed the zig-zag M1-M1' [010] rows of mixed cations around 2_1 axes at x = 0 (*e.g.*, Ag-Pb-Ag-Pb as the most probable sequence). However, we avoided the question of the spatial relation of the mixed (Ag, Pb) sites M2 to these mixed (Ag, Pb) positions M1: if in the latter sequence we select, *e.g.*, a certain site as Ag1, is the Ag2 polyhedron in the same level attached to it along the [102] direction or, along the [$\bar{1}$01] direction? These two configurational possibilities around every 2_1 axis at x = 0 are shown in Fig. 5 for two of the above derived space groups. When they are materialized at random, yet another polytype mechanism, *i.e.*, two positions of each M2-Sb1 layer against the adjacent M1-Sb3 layer, can be invoked, contributing to the polytypic character of diaphorite.

Each of the four possible MDO structures discussed above has two symmetry independent M1 and M2 sites (named M1, M1' and M2, M2'). To be in agreement with the observed family structure one M1 and one M2 site is occupied by Pb and the other by Ag.

Then the two distribution patterns
M1: Pb, M1': Ag, M2: Pb, M2': Ag
and
M1: Pb, M1': Ag, M2: Ag, M2': Pb
represent different polytypes.

Summary

The crystal structure of diaphorite consists of three types of stripes [001] of cation polyhedra: (a) stripes of alternating Pb1 and Ag4 sites, (b) double stripes of Sb polyhedra alternating with mixed (Pb,Ag) polyhedra, and (c) stripes of alternating Sb2 and Ag3 positions. The (a) and (b) stripes combine into (100) A layers whereas the (c) stripes alone form B layers in the structure. In the unit cell of diaphorite there are three planes on which polytypic phenomena can potentially occur:

(1) Planes (100) at x = 0.5 along which the adjacent A layers can assume two distinct positions *c*/2 apart, based on 2_1 and $\bar{1}$ operators (at x = 0.5) in the central, intervening B

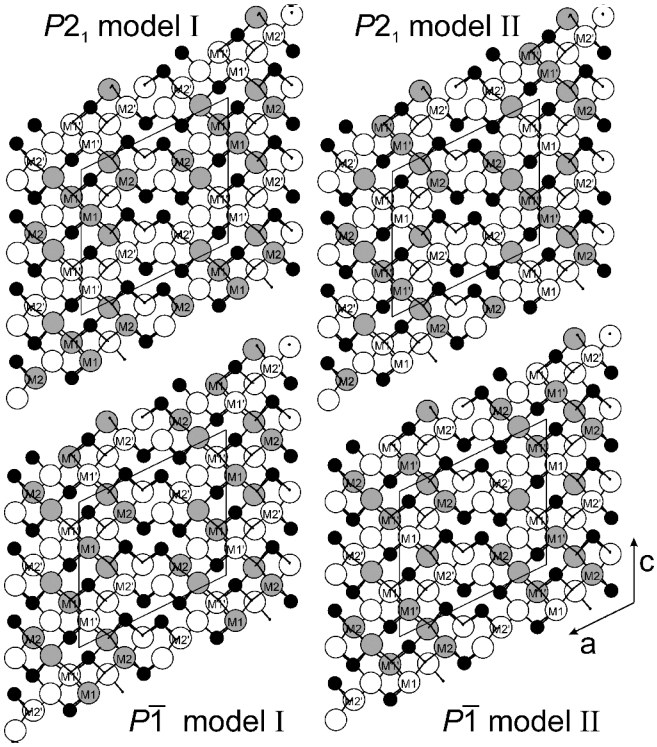

Fig. 5. Four hypothetical polytype variants of diaphorite. Pb sites are grey, Ag sites are white, Sb sites are black, S positions are represented by small dots. Only short cation-S bonds are shown. Examples are only presented for maximally ordered cases with simple *a*-axes, resulting in space groups $P2_1$ and $P\bar{1}$, respectively.

layer. These two alternatives form fully equivalent layer pairs A-B, *i.e.*, they also are crystal-chemically equivalent. Thus, they are true OD variants of an OD structure with two kinds of layers.

(2) Planes (100) at x = 0.0 where the adjacent halves of the layer A can assume two distinct positions differing by *c*/2, being alternatively related either by the 2_1 or the $\bar{1}$ operators (both at x = 0.0) of the **substructure**; these two polytypic variants are crystal-chemically non-equivalent.

(3) Planes (100) at x ≈ 0.2 on which two, in respect to Pb-Ag alternation ordered, component stripes of the (b) double-stripe (and the (100) slabs based on them) can assume two distinct mutual positions, *c*/2 apart. The resulting configurations of the A layer are crystal-chemically non-equivalent.

We assume that the probability of polytypic variations in the occupancy of selected cation sites in the structure of diaphorite decreases in the order (1) > (3) > (2). In addition, any non-stoichiometry in the Pb:Ag ratio will support creation of antiphase boundaries with a shift component of *c*/2 as a result of two adjacent Ag-Ag (or Pb-Pb) atoms occurring sporadically in each stripe of ordered Ag-Pb positions. All this might contribute to the attenuation of the weak diffraction phenomena expected for a structure with a pure OD character in cation positions.

Acknowledgements: This research was financed by the grant from the Danish Research Academy (Arhus) to J. Sejkora and by the grants RK99P03OMG003 (the State Department of Culture of the Czech Republic), and by the Swiss National Science Foundation (grant to T. A.: Crystal Chemistry of Minerals). Thorough reviews by Drs. S. Durovic, A. Meerschaut and Y. Moëlo were gratefully appreciated.

References

Balić-Žunić, T. & Makovicky, E. (1996): Determination of the centroid or 'the best centre' of a coordination polyhedron. *Acta Cryst.*, **B52**, 78–81.

Ďurovič, S. (1997): Fundamentals of OD theory. EMU Notes in Mineralogy, 1, 3–28. Ed. Merlino, S., Eötvös University Press, Budapest.

Enraf Nonius (1983): Structure determination package (SDP). Enraf Nonius, Delft, Holland.

Frizzo, P. & Simone, S. (1995): Diaphorite in the Pollone ore deposit (Apuan Alps – Tuscany, Italy). *Eur. J. Mineral.*, **7**, 705–708.

Hellner, E. (1958): Über komplex zusammengesetzte Spiessglanze III. Zur Struktur des Diaphorits, $Ag_3Pb_2Sb_3S_8$. *Z. Kristallogr.*, **110**, 169–174.

Hellner, E. & Burzlaff, H. (1964): Die Struktur des Smithits, $AgAsS_2$. *Naturwissenschaften*, **51**, 35–36.

Herbst-Irmer, R. & Sheldrick, G.M. (1998): Refinement of twinned structures with SHELX97. *Acta Cryst.*, **B54**, 443–449.

Hoffman, V., Trdlička, Z., Hulinský, V., Langrová, A., Arnoldová, V. (1977): Mineralogisch-chemisches Studium des Diaphorits von Kutná Hora (ČSSR). *Chem. Erde*, **36**, 36–44.

Ito, T. & Nowacki, W. (1974): The crystal structure of freieslebenite, $PbAgSbS_3$. *Z. Kristallogr.*, **139**, 85–102.

Makovicky, E. & Balić-Žunić, T. (1998): New measure of distortion for coordination polyhedra. *Acta Cryst.*, **B54**, 766–773.

Mozgova, N.N., Efimov, A.V., Nenasheva, S.N., Golovanova, T.I., Sivtsov, A.V., Tsepin, A.I., Dobretsova, I.G. (1989): New data on diaphorite and brogniardite. *Zapisky Vsesoyuznogo Mineral. Obshsch.*, **118/5**, 47–63 (in Russian).

Palache, C., Richmond, W.E., Winchell, A.N. (1938): Crystallographic studies of sulfosalts: baumhauerite, meneghinite, jordanite, diaphorite and freieslebenite. *Amer. Mineral.*, **23**, 821–836.

Sheldrick, G.M. (1997): SHELXL-97 and SHELXS-97. Programs for crystal structure determination. University of Göttingen, Germany.

Sveshnikova, O.L. & Borodayev, Yu.S. (1972): On the chemical composition of freieslebenite. *Trudy Mineralog. Mus. Akad. Nauk SSSR*, **21**, 133–138 (in Russian).

Wernick, J.H. (1960): Constitution of the $AgSbS_2$-PbS, $AgBiS_2$-PbS, and $AgBiS_2$-$AgBiSe_2$ system. *Amer. Mineral.*, **45**, 591–598.

Zepharovich, V. von (1871): Über Diaphorit und Freieslebenit. *Berichte Akad. Wiss. Wien, 1* . Abteilung, **63**, 130–156.

Received 2 November 2001
Modified version received 30 August 2002
Accepted 21 October 2002